Electrochemistry

DOI: 10.1002/anie.201308302

High-Power Electrochemical Energy Storage System Employing Stable Radical Pseudocapacitors**

Hitoshi Maruyama, Hideyuki Nakano, Masaaki Nakamoto, and Akira Sekiguchi**

Abstract: *The development of electrical energy storage devices that can operate at high charge and discharge rates is fundamentally important, however although electrochemical capacitors (ECs) can charge and discharge at high rates, their electrochemical storage capacity remains an order of magnitude lower than that of conventional lithium-ion batteries. Novel pseudocapasitors are developed, based on the stable persilyl-susbtituted free radicals of the heavy group 14 elements, ($tBu_2MeSi)_3E^{\bullet}$ [E = Si (**1**), Ge (**2**), and Sn (**3**)], as anode materials for energy storage system. Such systems showed a remarkable cycle stability without significant loss of power density, in comparison with similar characteristics of the known organic radical batteries, the dual carbon cell, and the electrochemical capacitor. Particularly important is that these novel electrochemical energy storage systems employing stable heavy group 14 element radicals are lithium-free. The electrochemical properties and structures of the reduced and oxidized species were studied by the cyclic voltammetry (CV), electron paramagnetic resonance (EPR) spectroscopy, and X-ray diffraction (XRD).*

The storage of electrical energy at high charge and discharge rates is a fundamentally important technology that is crucial for electric vehicles, both for the hybrid and plug-in hybrid types, as well as in power-grid applications.[1] Although electrochemical capacitors (ECs) that can charge and discharge at high rates are known, their electrochemical storage capacity remains an order of magnitude lower than that of conventional lithium-ion batteries.[2] Accordingly, extensive research efforts have been focused on increasing the energy density of ECs without sacrificing cycle life and high-power density. At present, depending on the charge-storage mechanism, ECs can be categorized into three types: electrochemical double-layer capacitors (EDLCs), pseudocapacitors, and hybrid capacitors. The drawback of the most commonly used EDLC, employing high-surface-area carbon-based active materials, is their low charge-storage capacity depending on the adsorption of ions.[3] Pseudocapacitors (or redox supercapacitors) for charge storage use fast and reversible surface (or near-surface) reactions. Transition-metal oxides, such as RuO_2,[4] Fe_3O_4,[5] and MnO_2,[6] as well as electrically conducting polymers,[7] are typical examples of pseudocapacitive-active materials. The latest type of EC, hybrid capacitors, combines a capacitive (or pseudocapacitive) electrode with a battery electrode, thus getting benefits from both capacitor and battery properties.[8] However, in the three above-mentioned EC systems, a reasonable compromise between the energy density and power density should be found. In particular, pseudocapacitors, based on the redox reactions used in their charge-storage mechanism, are often unstable during the cycling process and are yet to achieve power-density performances as high as those of ECs. A variety of radical compounds, such as open-shell molecules[9] and nitroxide radical polymers,[10] have been widely employed to achieve better stability and high-power performance. However, rather than achieving the goal of a completely rechargeable electrochemical energy storage system, these approaches pertained only to cathode materials. Accordingly, the development of anode materials is rather important for the development of stable high-power energy storage systems. In addition to this, a lithium-free electrochemical energy storage system is desirable because of the safety and resource issues.

Herein, we report novel pseudocapacitors, using stable persilyl-substituted free radicals based on the heavy group 14 elements, (tBu$_2$MeSi)$_3$E$^{\bullet}$ [E = Si (**1**), Ge (**2**), and Sn (**3**)],[11,12] as anode materials. The choice of such radicals was brought about by their ready reduction caused by the low reduction potentials (below −1.6 V vs. Ag/Ag^+[13]) and reversibility of the redox process, which makes these radical substances suitable candidates for EC anode materials. Moreover, given the long distance of 9.08 Å between the Si radical centers (seen in the crystal packing diagram of **1**, Figure 1), one can expect that these radicals will readily, and with very slight structural changes in the electrodes of the electrochemical devices, interact with other ionic species that can be introduced into the available space by electrochemical reduction.

Initially, we investigated the electrochemical properties of radicals **1**–**3** using cyclic voltammetry (CV). As the working electrodes, films of radicals **1**–**3** were prepared to coat a platinum electrode with each type of radical. As can be seen in the CV charts (Figure 2 a-1–c-1), the reduction and oxidation peaks were observed at about 1.2 and 2.0 V,

[*] H. Maruyama, Dr. M. Nakamoto, Prof. Dr. A. Sekiguchi
Department of Chemistry
Graduate School of Pure and Applied Sciences
University of Tsukuba, Tsukuba, Ibaraki 305-8571 (Japan)
E-mail: sekiguchi@chem.tsukuba.ac.jp
Homepage: http://www.chem.tsukuba.ac.jp/sekiguch/
Dr. H. Nakano
TOYOTA CENTRAL R&D LABS., INC.
Nagakute, Aichi 480-1192 (Japan)
E-mail: hnakano@mosk.tytlabs.co.jp

[**] Financial support from the Ministry of Education, Science, Sports, and Culture of Japan through the Grants-in-Aid for Scientific Research program (grant numbers 23550042, 24109006, and 24245007) is acknowledged.

Supporting information for this article is available on the WWW under http://dx.doi.org/10.1002/anie.201308302.

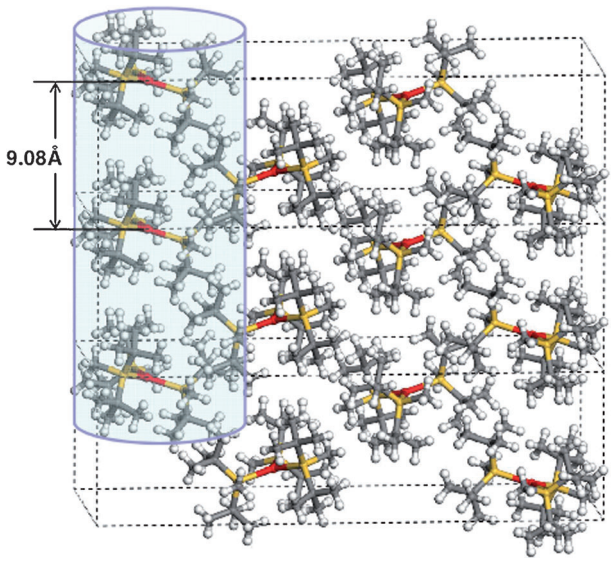

Figure 1. Crystal structure of **1**. The Si radical is stacked along the *a* axis to construct a pillar structure (blue part). Silicon radical, red; silicon, orange; carbon, gray; hydrogen, white.

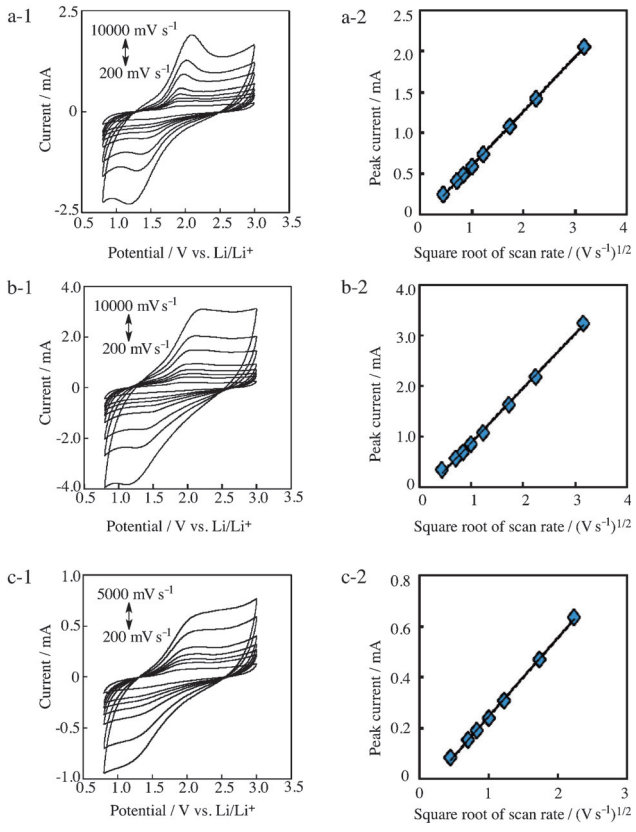

Figure 2. a-1–c-1) Cyclic voltammograms measured at sweep rates from 200 to 10000 (5000 for **3**) $mV s^{-1}$ in the potential range between 0.8 and 3.0 V, indicating the high-rate capability of radicals **1** (a-1), **2** (b-1), and **3** (c-1). a-2–c-2) Normalized peak current versus square root of the sweep rate for radicals **1** (a-2), **2** (b-2), and **3** (c-2). Lithium bis(trifluoromethylsulfonyl)imide (LiTFSI; 0.5 M) in *N*-methyl-*N*-propyl pyrrolidinium bis(trifluoromethylsulfonyl)imide (P13TFSI) was used as the electrolyte, and lithium metal was used as the counter electrode.

respectively. The positions of these peaks did not alter after multiple scans keeping the sweep rate constant, indicating the reversibility of the redox processes in the solid state. It should be noted that radicals **1**–**3** did not significantly dissolve in the electrolyte, because in the case of such an event the current peak is expected to decrease gradually and finally become unobservable.

Such insolubility of the electrochemically active species, radicals **1**–**3**, is fundamentally important for their use in electrochemical devices, such as EC electrodes. Furthermore, the peak positions did not change even at a higher sweep rate in the range of 0.2–10 $V s^{-1}$, indicating that a fast and reversible electron transfer occurred between the radicals and corresponding anions.

Figure 2 a-1–c-1 show the relation between sweep rate and peak current. Normalized peak currents i_p and the square root of the scan rate ($v^{1/2}$) show a linear relationship (Figure 2 a-2–c-2). From this linear dependence, the diffusion constants of radicals **1**–**3** were estimated as about 10^{-10} $cm^2 s^{-1}$, which is very close to that of nitroxide radicals (about 10^{-10} $cm^2 s^{-1}$).[14] These radical compounds exhibited much larger diffusion constants than those of the cathode-active materials commonly used in lithium-ion batteries (about 10^{-14} $cm^2 s^{-1}$),[15] suggesting that radicals **1**–**3** may possess high power and rapid charge–discharge properties. The peak separations at the same sweep rate followed the order **3** > **2** > **1**, implying that the reduction and oxidation reaction rates followed the reverse order, **1** > **2** > **3**. Accordingly, radicals **1**–**3** were found to be suitable candidates for use as anode materials in high-power electrochemical devices.

The theoretical capacities of radicals **1**–**3** were calculated to be 54, 49, and 45 mA h g^{-1}, respectively. Based on its largest capacity and fastest reaction rate among all three radicals, silyl radical **1** was chosen as the most suitable anode material. To investigate the electrochemical performance of the silyl radical battery (hereafter called **1**-cell), we prepared coin-type cells in which a mixture of **1** and carbon black was used as the anode, graphite as the cathode, and the ionic liquid *N*-methyl-*N*-propyl pyrrolidinium bis(trifluoromethylsulfonyl)imide (P13TFSI) as the electrolyte (Figure 3 a). The present electronic device does not require any metals such as lithium. The anode was prepared using 50 % of **1** and 45 % of carbon black along with 5 % of polytetrafluoroethylene as the binder. Carbon black was added to facilitate electron transfer from the active materials to the current collector and to provide cation absorbance sites similar to those in conventional ECs. Graphite, intercalating anions (such as PF_6^-, BF_4^-, and ClO_4^-) at high potentials up to 4.5 V versus Li/Li^+ (see Figure S1 in the Supporting Information), may thus serve as ideal cathode material for this cell system.[16] Because the electrolyte commonly used in ECs, triethylmethylammonium tetrafluoroborate,[17] is not inert toward radicals **1**–**3**, reacting with them through a halogen-abstraction reaction, we employed a halogen-free ionic liquid as the electrolyte. In this system, the charge–discharge behavior in the potential range 0.0–3.8 V was measured.

To probe further the electrochemical reversibility of the cell (Figure 3 a) and reconfirm the redox mechanism of radicals **1**–**3**, we monitored starting (red), fully reduced

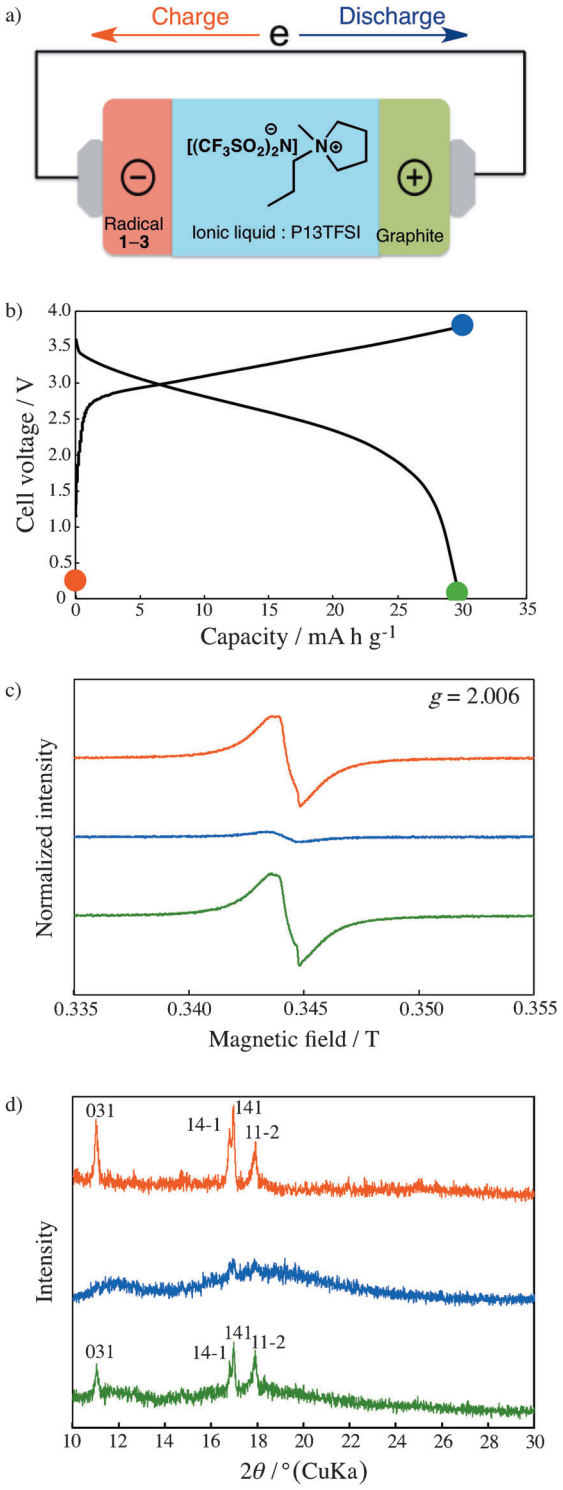

Figure 3. a) Schematic representation of a radical **1**-cell. The average cell potential is calculated to be about 3 V from each electrode redox potential. b) First charge–discharge curves of **1**-cell at 1 C rate between 0.0 and 3.8 V. The color code everywhere is: starting (red), reduced (blue), and oxidized (green) materials. c) EPR spectra and d) XRD patterns showing the reversibility of the reduction (charge)–oxidation (discharge) process and *N*-methyl-*N*-propyl pyrrolidinium cation attaching–detaching process in **1**-cell as shown by the potential curve in (b). XRD diffraction peaks are indexed using single-crystal data.[11a]

(blue), and oxidized (green) electrodes made of **1**. Figure 3b shows the first-cycle charge–discharge curves for **1**-cell. The capacity was calculated on the basis of the total weight of the anode. Thus, **1**-cell is a hybrid system in which the electrochemical storage could be achieved by both the redox reaction of **1** and surface ion adsorption on carbon black. The calculated initial discharge capacity and energy density of **1**-cell were 30 mA h g^{-1} and 74 mW h g^{-1}, respectively, whereas those of the dual carbon cell were 20 mA h g^{-1} and 45 mW h g^{-1}, respectively (see Figure S2 in the Supporting Information). The reversible redox capacity of **1** was calculated to be 71 % of the capacities of both devices.

In the electron paramagnetic resonance (EPR) experiments (Figure 3c), the starting sample exhibited a strong isotropic signal ($g = 2.006$); however, no signal could be observed after reduction (charge). Upon the subsequent oxidation (discharge) of the reduced species, the signal corresponding to the starting radical appeared again, further confirming the reversibility of the reduction–oxidation process. In such electrochemical processes, reduction implies the transformation of radical **1** to the corresponding silyl anion, and oxidation means the reverse transformation of the silyl anion into the starting radical **1**, as depicted in Scheme 1. This

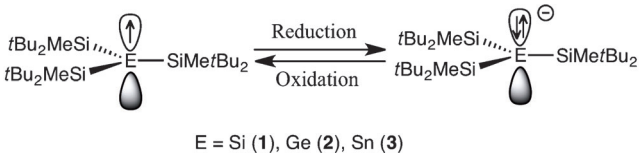

Scheme 1. Reversible electrochemical anodic reduction–oxidation process of radicals **1**–**3**.

remarkable reversibility persisted without any changes during electrochemical reduction and oxidation at room temperature, thus demonstrating the stability of the Si radical. During the test, the ratio of the EPR signal intensities was as follows: starting radical **1**:reduced species:oxidized species = 1.0:0.2:1.0. This result indicates that the initially generated silyl anions were formed up to 80 % upon reduction, and their subsequent oxidation regenerated the starting silyl radicals.

The structures of the reduced and oxidized samples were investigated by X-ray diffraction (XRD; Figure 3d). The peaks of the starting sample were assigned on the basis of the previously reported single-crystal lattice constant.[11a] After reduction, the XRD pattern of **1** dramatically changed as the peaks disappeared, thus indicating that the structure of **1** was mostly disordered and became gel-like upon reduction, generating silyl anions that interacted with the bulky cationic parts of the ionic liquid. Notably, the fully oxidized material shows an XRD pattern that nearly superimposes on the starting materials, unambiguously indicating a fully reversible reduction–oxidation process. By using lithium bis(trifluoromethylsulfonyl)imide (LiTFSI) as the electrolyte, **1** was converted to the silyllithium derivative upon reduction (Figure S3). The observed XRD peaks agreed well with those previously reported.[18] Furthermore, silyl radical **1** remained insoluble in the electrolyte during the reduction–oxidation

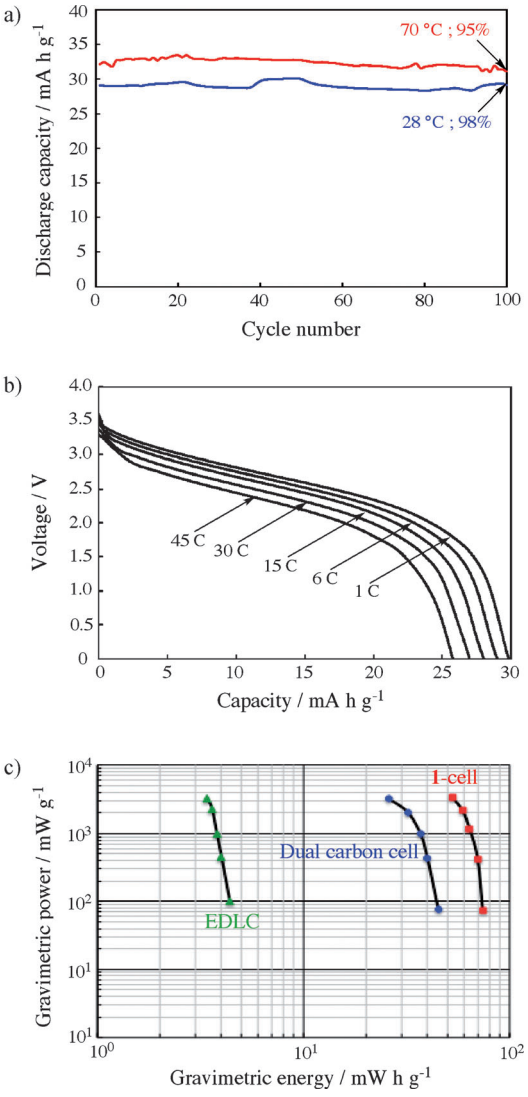

Figure 4. a) Cycle performance of discharge processes of **1**-cell between 0.0 and 3.8 V at 28 (blue) and 70 °C (red) at a constant current 1 C rate (32 mA h g^{-1}). b) Discharge curves at various C rates for **1**-cell: in the rate test, the cell was charged at 1 C to 3.8 V and discharged at different rates. c) Ragone plots for **1**-cell, the dual carbon cell, and other EDLCs: the energy and power densities were calculated using the electrode weight.

process, which enables its application as an electrode-active material. Thus, all of the above-discussed CV, EPR, and XRD measurements unambiguously confirmed the full reversibility of the reduction–oxidation processes in **1**-cell.

Figure 4 shows the electrochemical performance of **1**-cell. To assess their stability, the **1**-cells were cycled at 28 °C, and as shown in Figure 4a (blue), the capacity remained at 98 % of the first-cycle capacity after 100 cycles. In addition, to assess the high-temperature performance, we selected aggressive test conditions wherein the cell was cycled at 70 °C. The capacity was as high as 95 % after 100 cycles (Figure 4a, red). These results indicate that **1** did not decompose or dissolve even at elevated temperatures. In contrast, the capacity of a nitroxide radical polymer battery was 45 % of the first-cycle capacity after 100 cycles at 60 °C.[19] We thus concluded that a battery using both **1** and the corresponding silyl anion should have high thermal stability. Radical materials are known to exhibit a high-rate performance, and accordingly our radical-containing electrodes also demonstrated outstanding high-rate capability. The C rate dependence of the discharge curves for **1**-cell was investigated at 1–45 C (Figure 4b). The C rate corresponds to a full discharge after 1/C h. Even at 45 C, which corresponds to a time of 80 s for full discharge, the capacity was 87 % of that at 1 C, implying that **1**-cell is suitable for high-power applications. This result clearly indicates that the cations (*N*-methyl-*N*-propyl pyrrolidinium ion) in the electrode can rapidly reach the active radical anode material. We also used germyl radical **2** and stannyl radical **3** as active anode materials (Figures S4-a and S5-a show the first charge–discharge curves at 0–3.8 V). The capacity and energy density of **2** and **3** were 27 mA h g^{-1} and 66 mW h g^{-1}, and 26 mA h g^{-1} and 61 mW h g^{-1}, respectively. About 70 % of the calculated capacities of **2** and **3** were reversibly reduced/oxidized in these batteries; furthermore, these capacities were as high as 95 % after 100 cycles. These radicals also exhibited good cycle performance compared with **1** (Figures S4-b and S5-b). For practical applications, a compromise between power and energy density is important and is often represented in a Ragone plot (Figure 4c). For comparison, we also measured the behavior of a dual carbon cell (carbon black anode, graphite cathode, and P13TFSI electrolyte) and an EDLC (carbon black anode, carbon black cathode, and P13TFSI electrolyte). Both of these ECs were fabricated with anode (2 mg) and cathode (4 mg) compositions similar to that of **1**-cell. Most EC materials show a substantial decrease in the specific energy densities (4.4 mW h g^{-1}), thus making them less useful in applications, such as electric and hybrid electric vehicles and power tools that require high capacities. In contrast, **1**-cell and the dual carbon cell have larger energy densities at 1 C rate (**1**-cell: 74 mW h g^{-1}, dual carbon cell: 45 mW h g^{-1}). Figure 4c shows that **1**-cell clearly retains its energy storage capacity even at the very high rate required for such applications. At 80 s (45 C rate), the charge–discharge rate, **1**-cell (53 mW h g^{-1}) delivers almost twice the energy density of the dual carbon cell (26 mW h g^{-1}) and 15 times larger energy density than the EDLC (3.4 mW h g^{-1}). This high-rate performance of **1**-cell originates from the fast ion diffusion of the radical compounds and the rate of the interchange between radical **1** and the corresponding anion, as shown in Scheme 1.

In this study we demonstrated that our silyl (or germyl and stannyl) radical batteries (lithium-free batteries) revealed remarkable cycle stability without significant loss of high-power density, particularly at higher temperatures, as compared with analogous characteristics of the previously reported organic radical batteries, the dual carbon cell, and the EDLC. The present electrochemical energy storage system employing stable heavy group 14 element radicals does not require any metals such as lithium.

Experimental Section

Cyclic voltammograms: Radicals **1**–**3**[11a,c] were coated on platinum (about 0.1 cm^2). Hermetically sealed two-electrode cells were used for

the electrochemical tests. The electrodes were separated from the lithium counter electrode using a porous polyethylene film impregnated with 0.5 M lithium bis(trifluoromethylsulfonyl)imide (LiTFSI)/*N*-methyl-*N*-propyl pyrrolidinium bis(trifluoromethylsulfonyl)imide (P13TFSI). The three layers were pressed between two current collectors, one in contact with the cathodic material and the other in contact with the anodic material.

Cell fabrication: Anodes were prepared by mixing radicals **1**–**3** and carbon black (ECP) with polytetrafluoroethylene (PTFE) as a binder (ratio: 0.50:0.45:0.05). Cathodes were prepared by mixing graphite with PTFE as a binder (ratio: 0.9:0.1). These materials (anode: 2 mg, cathode: 4 mg) were coated onto a stainless steel mesh. The anodes impregnated with the electrolyte were separated from the graphite cathodes by a porous polyethylene film impregnated with P13TFSI.

Electrochemical characterization: The CV and the charge-discharge properties were measured using HZ5000 and HJ1010 mSM8A instruments (Hokuto), respectively. All tests were performed in the voltage range of 0.8–3.0 V versus Li/Li^+ at 25 °C. All tests of the charge–discharge properties were performed in the voltage range of 0.0–3.8 V.

EPR measurements: Anodic measurements were performed using an EMX Plus spectrometer (Bruker, 9.62 GHz) in an argon atmosphere at room temperature.

XRD measurements: XRD patterns were obtained using a Rint-TTR instrument (Rigaku, Japan). All measurements were conducted in an argon atmosphere at room temperature using CuKα radiation.

Received: September 23, 2013
Published online: December 18, 2013

Keywords: electrochemistry · electrode materials · heavier group 14 elements · radicals · secondary battery

[1] a) B. Kang, G. Ceder, *Nature* **2009**, *458*, 190 – 193; b) Y. K. Sun, S. T. Myung, B. C. Park, J. Prakash, I. Belharouak, K. Amine, *Nat. Mater.* **2009**, *8*, 320 – 324.
[2] a) P. Simon, Y. Gogotsi, *Nat. Mater.* **2008**, *7*, 845 – 854; b) J. R. Miller, P. Simon, *Science* **2008**, *321*, 651 – 652.
[3] a) J. Chmiola, G. Yushin, Y. Gogotsi, C. Portet, P. Simon, P. L. Taberna, *Science* **2006**, *313*, 1760 – 1763; b) T. Brezesinski, J. Wang, S. H. Tolbert, B. Dunn, *Nat. Mater.* **2010**, *9*, 146 – 151.
[4] a) W. Sugimoto, H. Iwata, Y. Yasunaga, Y. Murakami, Y. Takasu, *Angew. Chem.* **2003**, *115*, 4226 – 4230; *Angew. Chem. Int. Ed.* **2003**, *42*, 4092 – 4096; b) V. Augustyn, J. Come, M. A. Lowe, J. W. Kim, P. L. Taberna, S. H. Tolbert, H. D. Abruña, P. Simon, B. Dunn, *Nat. Mater.* **2013**, *12*, 518 – 522.
[5] N.-L. Wu, *Mater. Chem. Phys.* **2002**, *75*, 6 – 11.
[6] T. Brousse, M. Toupin, R. Dugas, L. Athouël, O. Crosnier, D. Bélanger, *J. Electrochem. Soc.* **2006**, *153*, A2171 – A2180.
[7] A. Rudge, I. Raistrick, S. Gottesfeld, J. P. Ferraris, J. Power, *Sources* **1994**, *47*, 89 – 107.
[8] K. Naoi, P. Simon, *Electrochem. Soc. Interface* **2008**, *17*, 34 – 37.
[9] Y. Morita, S. Nishida, T. Murata, M. Moriguchi, A. Ueda, M. Satoh, K. Arifuku, K. Sato, T. Takui, *Nat. Mater.* **2011**, *10*, 947 – 951.
[10] T. Suga, S. Sugita, H. Ohshiro, K. Oyaizu, H. Nishide, *Adv. Mater.* **2011**, *23*, 751 – 754.
[11] For Si and Ge radicals, see: a) A. Sekiguchi, T. Fukawa, M. Nakamoto, V. Ya. Lee, M. Ichinohe, *J. Am. Chem. Soc.* **2002**, *124*, 9865 – 9869; b) G. Molev, B. Tumanskii, D. Sheberla, M. Botoshansky, D. Bravo-Zhivotovskii, Y. Apeloig, *J. Am. Chem. Soc.* **2009**, *131*, 11698 – 11700; For the Sn radical, see: c) A. Sekiguchi, T. Fukawa, V. Ya. Lee, M. Nakamoto, *J. Am. Chem. Soc.* **2003**, *125*, 9250 – 9251.
[12] Recent reviews of heavier group 14 element radicals: a) P. P. Power, *Chem. Rev.* **2003**, *103*, 789 – 809; b) V. Ya. Lee, A. Sekiguchi, *Eur. J. Inorg. Chem.* **2005**, 1209 – 1222; c) V. Ya. Lee, A. Sekiguchi, *Acc. Chem. Res.* **2007**, *40*, 410 – 419; d) V. Ya. Lee, A. Sekiguchi, *Organometallic Compounds of Low-Coordinate Si, Ge, Sn, and Pb. From Phantom Species to Stable Compounds*, Wiley, Chichester, **2010**, chap. 2.
[13] J. Y. Becker, V. Ya. Lee, M. Nakamoto, A. Sekiguchi, A. Chrostowska, A. Dargelos, *Chem. Eur. J.* **2009**, *15*, 8480 – 8484.
[14] N. Sano, W. Tomita, S. Hara, C. M. Min, J. S. Lee, K. Oyaizu, H. Nishide, *ACS Appl. Mater. Interfaces* **2013**, *5*, 1355 – 1361.
[15] D. Y. W. Yu, C. Fietzek, W. Weydanz, K. Donoue, T. Inoue, H. Kurokawa, S. Fujitania, *J. Electrochem. Soc.* **2007**, *154*, A253 – A257.
[16] a) H. Wang, M. Yoshio, *Chem. Commun.* **2010**, *46*, 1544 – 1546; b) R. Santhanam, M. Noel, *J. Power Sources* **1998**, *76*, 147 – 152; c) J. R. Dahna, J. A. Seel, *J. Electrochem. Soc.* **2000**, *147*, 899 – 901.
[17] K. Naoi, S. Ishimoto, J. Miyamoto, W. Naoi, *Energy Environ. Sci.* **2012**, *5*, 9363 – 9373.
[18] M. Nakamoto, T. Fukawa, V. Ya. Lee, A. Sekiguchi, *J. Am. Chem. Soc.* **2002**, *124*, 15160 – 15161.
[19] K. Nalahara, K. Oyaizu, H. Nishide, *Chem. Lett.* **2011**, *40*, 222 – 227.

